ANNALS of the ORADEA UNIVERSITY.

Fascicle of Management and Technological Engineering, Volume VII (XVII), 2008

CRACK CENTRE DEPTH AND RESIDUAL TENSIONS INFLUENCE ON STRESS INTENSITY FACTOR MODE I VARIATION IN THE HERTZIAN STRESSES FIELD OF GEAR TEETH

Claudiu Ovidiu POPA, Lucian Mircea TUDOSE
Technical University of Cluj – Napoca

Keywords: fatigue cracks, stress intensity factor K_I, crack centre depth, residual tensions

Abstract: A detailed analysis of Hertzian stresses in the substrate of the meshing spur gear with internal fatigue crack was presented. The most outstanding parameter that governs the fatigue crack growth under tensile stress field is the stress intensity factor, mode I, K_I. This is a sufficient parameter to describe the whole stress field at the crack tip. An accurate stress intensity factor K_I evolution was worked out taking into account the position of the crack centre depth, and also, the residual tensions that act on the surface of the tooth, tensions that are linearly decreasing with the depth in the contact zone.

1. INTRODUCTION

From the engineering point of view no reliable lifetime prediction method exists, which would enable the life expectancy of structures to be calculated with sufficient accuracy. One of the primary drawbacks of current approaches is their obvious inability to adequately include into an engineering calculation scheme basic knowledge of the microstructural response to cyclic loads during each of the stages of the fatigue process and, however, most service loads are far from constant amplitude loads, often resulting in large systematic errors in life predictions. A typical curve which presents the correlation between tensions and number of cycles to fracture is the *Wőhler curve* also named the *S-N curve*. It is a graph of the magnitude of a cyclical stress against the logarithmic scale of cycles to failure, N_f. An example, for OLC45 (AISI 1045) was presented in Fig. 1a [11].

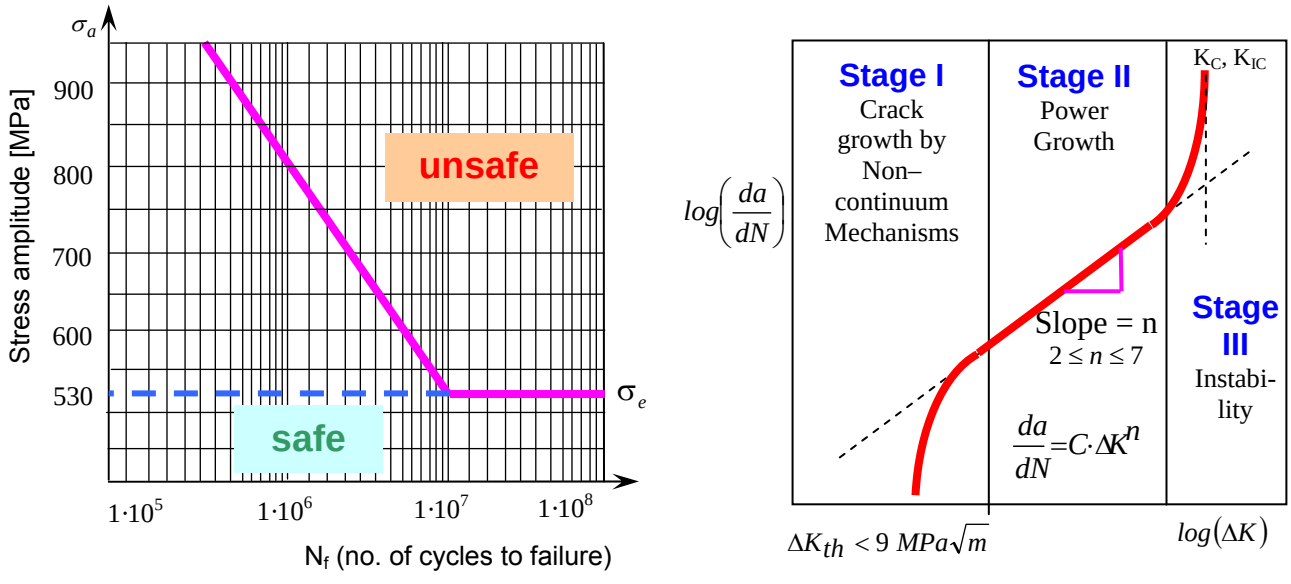

a. **b.**

Fig.* 1*: Fatigue behavior of metallic components:* a *– Wőhler curve for OLC 45 (AISI 1045);* b *– fatigue crack propagation stages

In order to determine the life prediction with a greater accuracy, fracture mechanics considers that there are three stages that govern the fatigue behavior of the component, namely: crack initiation, long crack propagation and final fracture (Fig. 1b) [16].

The stage I (Fig. 1b) [7][12][16] corresponds to *nucleation* and *small crack growth* of the fatigue crack; it depends on the material microstructure, the applied stress ratio and the environment.

Fatigue process in Stage II is hight as the *power growth* behavior (usually characterized by the Paris law), corresponding to a *stable crack growth*; it slightly depends on the parameters in Stage I. Here, C and n are material constants that can be obtained from the intercept and slope of the linear log (da/dN) versus log (ΔK) plot (Fig. 1b).

The curve shown is bounded by two limits, the upper one being the fracture toughness of the material K_C (or K_{IC}) and the lower limit being the fatigue crack threshold ΔK_{th} [6], the asymptotic value of ΔK at which the crack growth per cycle da/dN approaches to zero.

Considering a structure in which a crack develops, due to the application of repeated loads or due to a combination of loads and environmental attack this crack will growth in time. The longer the crack, the higher the stress concentration induced by it. This implies that the rate of crack propagation will increase with time.

The last stage (instability) corresponds to a dramatic growing of the crack that has as result, eventually, the fracture of the component.

2. STRESS INTENSITY FACTOR MODE I (K_I) RELEVANCE IN THE FATIGUE CRACK BEHAVIOR

The fracture mechanics approach is based on the assumption that the crack tip conditions are uniquely defined by a single loading parameter, the *stress intensity factor*, (SIF) noted *K.* This is one of the most important parameter that governs stage II (stable crack growth).

In the elastic case LEFM (Linear Elastic Fracture Mechanics), the SIF is a sufficient parameter to describe the whole stress field at the tip of the crack and when the size of the plastic zone at the crack tip is small compared to the crack length, the SIF may still give a good indication of the stress environment of the crack tip.

There are three basic types of crack growth modes, each one being governed by a certain SIF as shown in Fig. 2 [1][2][4][7].

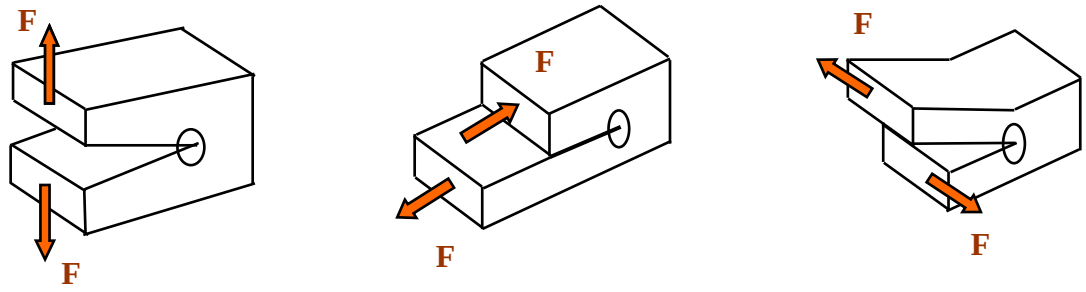

a. **b.** **c.**

Fig. 2: Basic crack extensions modes: **a –** ***Mode I*****; b –** ***Mode II*****; c –** ***Mode III***

Stress intensity factor K_I is responsible for mode I, also known as *extension mode* (Fig. 2 a), K_{II} for mode II, named *sliding mode* (Fig. 2b) and K_{III} for mode III, known as *tearing mode* (Fig. 2c).

If the material is supposed to a tensile stress, fact that corresponds to a positive value of K_I, the crack faces are growing in concordance with mode I. If there are compressive tensions in the local contact zone, the stress intensity factor K_I values are

negative, fact that produces the compression of the crack faces, meaning that the crack development under this mode is obstructed.

In the particular LEFM approach, the relationship between the SIF and crack growth per cycle was, generally, established in concordance with the *Paris law* [2][3][5][13][16]:

$$da / dN = C \cdot \Delta K_I{}^n \tag{1}$$

where: a – crack length, mm;

N – number of loading cycles;

da/dN – crack growth per cycle, mm/cycle;

ΔK_I – stress intensity factor range, MPa·(mm)$^{1/2}$:

$$\Delta K_I = K_{I\max} - K_{I\min} = \beta \cdot \Delta s \cdot \sqrt{a} \tag{2}$$

Δs – stress range, MPa;

β – constant depending on the geometry of the body;

n – Paris law exponent;

C – Paris Law coefficient, (mm/cycle)/[MPa·(mm)^{½}]^n;

The number of cycles necessary for a crack to grow from an initial length, a_i, to a final length, a_f, obtained from equation 1 is:

$$N_p = \int dN = \int_{a_i}^{a_f} \frac{da}{C[\Delta K_I(a)]^n} \tag{3}$$

3. STRESS FIELD IN THE PINION TOOTH SUB-SURFACE

The relationship between the contact point coordinate on the pitch line (the system originated in A and oriented towards N_2, along the pitch line) and the corresponding point coordinate on the surface of the involute tooth (the system XAY, originated in the point A and orientated towards E, along the tooth profile) is (Fig. 3a) [14]:

$$x_{pl}(X) = -N_1A + \sqrt{N_1A^2 + X_{contact} \cdot d_{b1}} \tag{4}$$

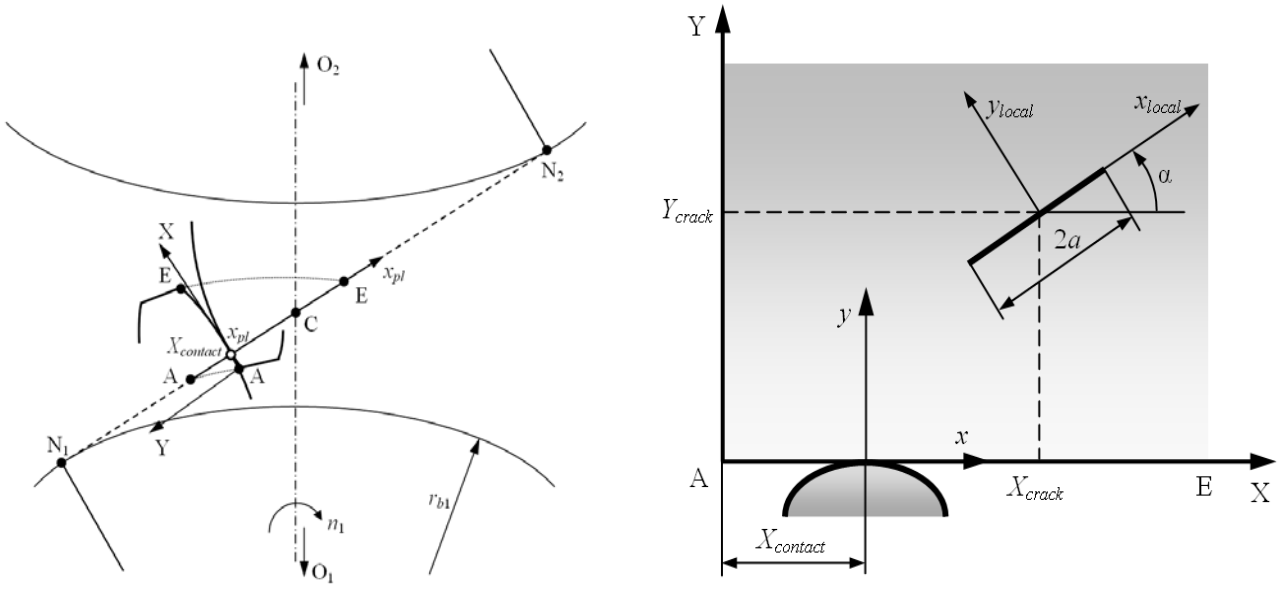

a. **b.**

Fig. 3: Coordinate systems:* a *– along pitch line;* b *– on contact zone

In Fig. 3a, N_1N_2 represents the pitch line, A (gearing entrance point), C (pitch point), E (gearing outgo point) are the mashing characteristic points, N_1A – curvature radius of involute at point A, mm, d_{b1} – base diameter of pinion, mm.

The surface and the sub-surface of the contact zone between points A and E corresponding to pitch line is considered on the pinion tooth (Fig. 3b). The coordinate system AXY is the same as the system AXY presented in Fig. 3a.

The position of the current contact point is determined by the abscissa $X_{contact}$.

In the current contact point a local system *xy* is also anchored (Fig. 3b) [14].

On contact zone act simultaneously a normal force and a frictional force.

Any point of material is subjected to normal and shear stresses due to Hertzian and frictional stresses.

We considered two mashing spur gears made of OLC45 (AISI 1045); the input data of the gearing are shown in Tab. 1.

Description	Denotation	Value	M.U.
Module	m	2.5	mm
No. of pinion teeth	z_1	64	-
No. of wheel teeth	z_2	74	-
Addendum modif. coefficients	x_1	0	-
	x_2	0	-
Engine power	P	8.5	kW
No. of revolutions of pinion shaft	n_1	930	rpm
Width of pinion	b_w	8.2	mm
Radial contact ratio	ε_α	1.804	-
Normal force	F_n	2,526	N
Linear load	q	308	N/mm

Tab.1. Gearing input data

The normal and shear stresses due to Hertzian load can be expressed [9][10][14]:

$$\sigma_{xH} = \begin{cases} \dfrac{-\sigma_H \cdot y}{b}\left[\sqrt{\dfrac{b^2+t}{t}}\cdot\left(2-\dfrac{b^2y^2}{t^2+b^2y^2}\right)-2\right] & \text{if } y \neq 0 \\ -\sigma_H \cdot \sqrt{1-\left(\dfrac{x}{b}\right)^2} & \text{if } y = 0 \wedge |x| \leq b \\ 0 \text{ if } y = 0 \wedge |x| > b \end{cases} \quad (5)$$

$$\sigma_{yH} = \begin{cases} \dfrac{-\sigma_H \cdot by^3}{t^2 + b^2 y^2} \cdot \sqrt{\dfrac{b^2 + t}{t}} \ if \ \ y \neq 0 \\ -\sigma_H \cdot \sqrt{1 - \left(\dfrac{x}{b}\right)^2} \ if \ \ y = 0 \cap |x| \leq b \\ 0 \ if \ \ y = 0 \cap |x| > b \end{cases} \tag{6}$$

$$\tau_{xy} = \begin{cases} \dfrac{-\sigma_H \cdot bxy^2}{t^2 + b^2 y^2} \cdot \sqrt{\dfrac{t}{b^2 + t}} \ if \ \ y \neq 0 \\ 0 \ if \ \ y = 0 \end{cases} \tag{7}$$

where: $$t = \frac{x^2 + y^2 - b^2 + \sqrt{\left(x^2 + y^2 - b^2\right)^2 + 4b^2 y^2}}{2} \tag{8}$$

If μ_f is the frictional coefficient between the two teeth in contact and the tangential force on the contact surface is (according to the Coulomb law) proportional to the normal acting force, the stresses due to frictional forces are given by the equations [4][14]:

$$\sigma_{xf} = \begin{cases} 2\mu_f \sigma_H \cdot \dfrac{x}{b}\left(1 - \sqrt{\dfrac{t}{b^2 + t}} - \dfrac{xyb^2}{t^2 + b^2 y^2} \cdot \dfrac{t}{b^2 + t}\right) if \ \ y \neq 0 \\ 2\mu_f \sigma_H \cdot \dfrac{x}{b} \ if \ \ y = 0 \cap |x| \leq b \\ 2\mu_f \sigma_H \cdot \left[\dfrac{x}{b} - \sqrt{\left(\dfrac{x}{b}\right)^2 - 1}\right] if \ \ y = 0 \cap |x| > b \cap x > 0 \\ 2\mu_f \sigma_H \cdot \left[\dfrac{x}{b} + \sqrt{\left(\dfrac{x}{b}\right)^2 - 1}\right] if \ \ y = 0 \cap |x| > b \cap x < 0 \end{cases} \tag{9}$$

$$\sigma_{yf} = \mu_f \cdot \tau_{yxH}$$

$$\tau_{yxf} = -\mu_f \cdot \sigma_{xH}$$

where *x* and *y* represent the coordinates of the considered point in the local system of coordinates *xy* attached to the actual contact point (Fig. 3b).

All these stresses are functions of $X_{contact}$, X_{crack}, Y_{crack}, x_{local} and inclination angle α.

Effective stresses in any point of the active surface or of its sub-surface of the pinion tooth with taking into account the residual stresses (which are linearly decreasing with the depth in the contact zone) can be determine by the following equations [14]:

$$\begin{aligned} \sigma_x &= \sigma_{xH} + \sigma_{xf} + q_{xrez} \\ \sigma_y &= \sigma_{yH} + \sigma_{yf} \\ \tau_{yx} &= \tau_{yxH} + \tau_{yxf} \end{aligned} \tag{10}$$

The normal and shear stresses that load both sides of the crack (Fig. 4) according to rotated system $x_{local}y_{local}$ are [14]:

$$\sigma_{xlocal} = \frac{1+\cos(2\alpha)}{2}\sigma_x + \frac{1-\cos(2\alpha)}{2}\sigma_y + \sin(2\alpha)\tau_{yx}$$
$$\sigma_{ylocal} = \frac{1-\cos(2\alpha)}{2}\sigma_x + \frac{1+\cos(2\alpha)}{2}\sigma_y - \sin(2\alpha)\tau_{yx} \quad (11)$$
$$\tau_{yxlocal} = \frac{-\sin(2\alpha)}{2}\sigma_x + \frac{\sin(2\alpha)}{2}\sigma_y + \cos(2\alpha)\tau_{yx}$$

Using equations 11 one can determine the values of normal and shear stresses in every point belonging to the crack (in crack coordinate system), for any crack position inside the material (X_{crack}, Y_{crack}), for any length (2a) and inclination angle (α), and for any position of contact point ($X_{contact}$).

Let assume that in the substrate of the pinion tooth there exists an internal crack of 2*a* length and whose both faces are loaded by normal and tangential stresses of arbitrary intensity, as shown in Fig. 4.

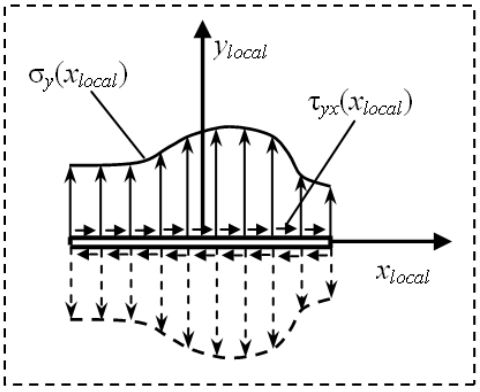

Fig. 4: General loading on internal crack surfaces

The position of the crack is given by the coordinates X_{crack} and Y_{crack} of its centre in the system AXY (Fig. 6). Affined to crack, a local coordinate system $x_{local}y_{local}$ is defined. This system is originated in the centre of the crack. Note that the range of abscissa x_{local} is [– *a*, *a*] and the ordinate y_{local} = 0.

The most general case presume that the crack is inclined with angle α with respect of axis AX (angle between the *X* and x_{local} directions, measured counterclockwise) as shown in Fig. 3 b. The stress intensity factor mode I can be determined by expression [14]:

$$K_I = \frac{1}{\sqrt{\pi \cdot a}} \cdot \int_{-a}^{a} \sigma_{ylocal} \cdot \sqrt{\frac{a + x_{local}}{a - x_{local}}} dx_{local} \quad (12)$$

4. INFLUENCES OF CRACK CENTRE DEPTH AND RESIDUAL TENSIONS ON STRESS INTENSITY FACTOR K_I VALUES

In order to study the SIF variation mode I, K_I, we considered an internal crack situated at the point having X_{crack} = 2.0 mm and the semilength *a* = 0.05 mm.

We also considered that the centre depth is variable (Y_{crack}= 0.2, 0.3, 0.5 and 0.6 mm) and that the crack is subjected to the Hertzian and frictional stresses (determined for μ_f = 0.1) with taking account the variable residual tensions (q_{rez} = 0, 100, 200, 400 MPa).

Based on equations 11 and 12 we compute the values of SIFs K_I for digitized (with the step π/6) values of the inclination angle α of the crack (Fig. 5).

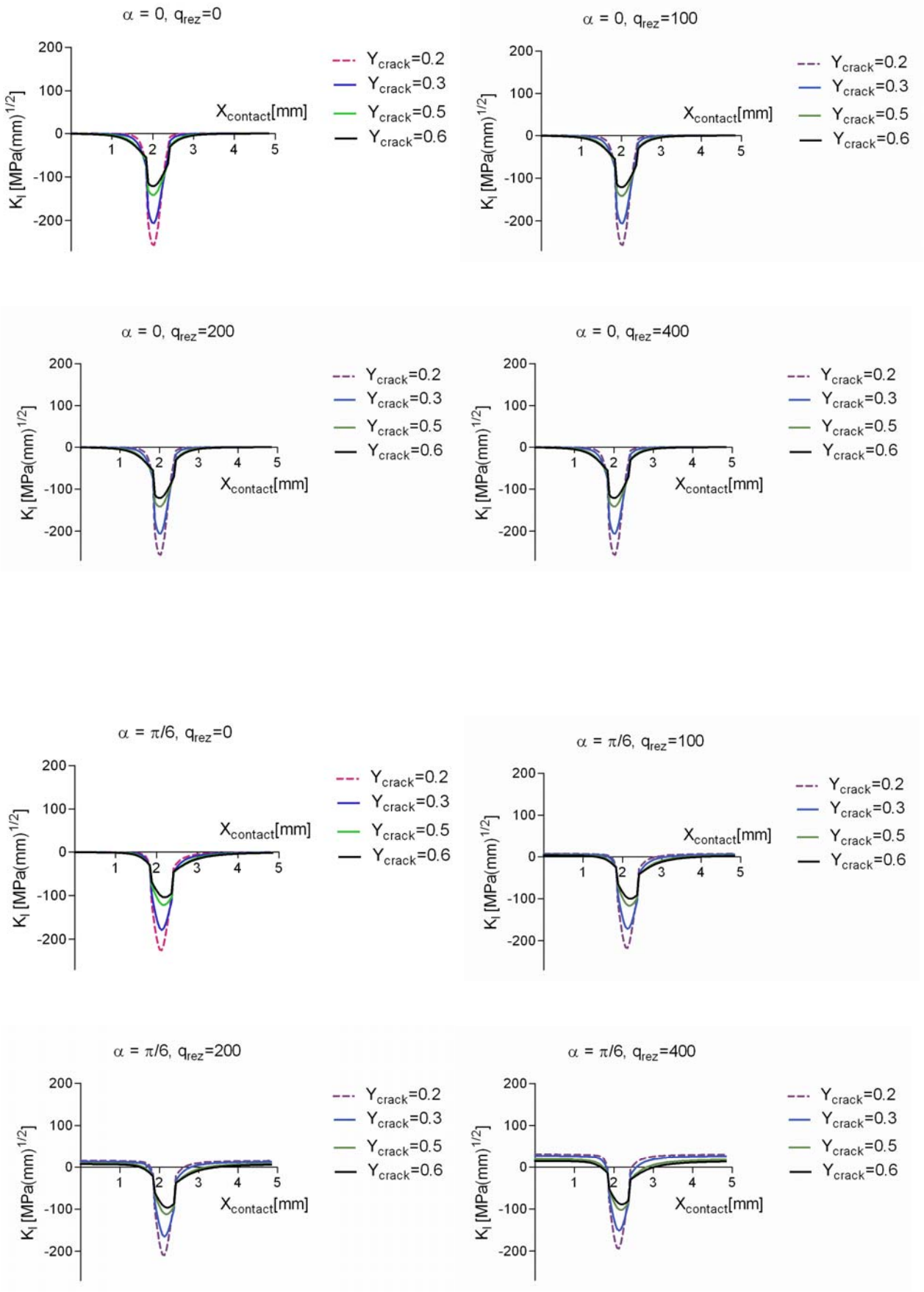
α = 0, q_rez=0
α = 0, q_rez=100
α = 0, q_rez=200
α = 0, q_rez=400
α = π/6, q_rez=0
α = π/6, q_rez=100
α = π/6, q_rez=200
α = π/6, q_rez=400
K_I [MPa(mm)^1/2]
X_contact[mm]
Y_crack=0.2
Y_crack=0.3
Y_crack=0.5
Y_crack=0.6

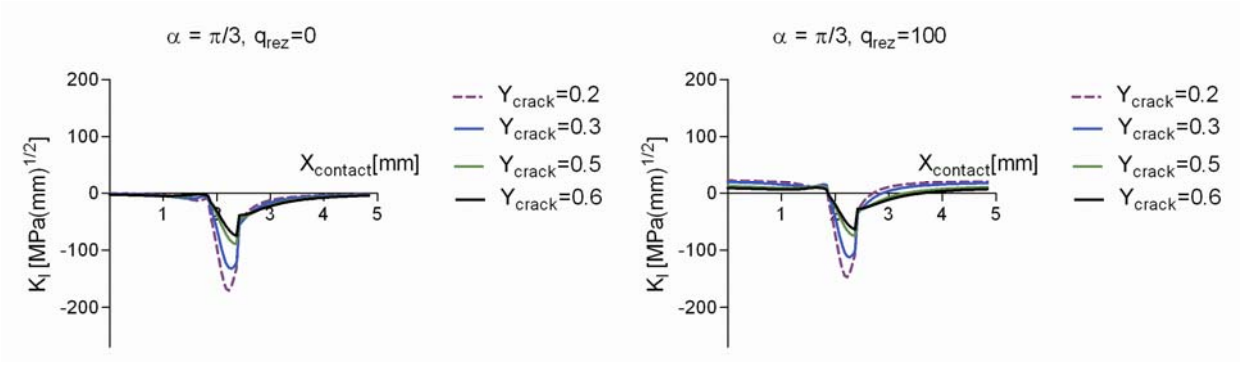
α = π/3, q_rez=0
α = π/3, q_rez=100
K_I [MPa(mm)^1/2]
X_contact[mm]
Y_crack=0.2
Y_crack=0.3
Y_crack=0.5
Y_crack=0.6

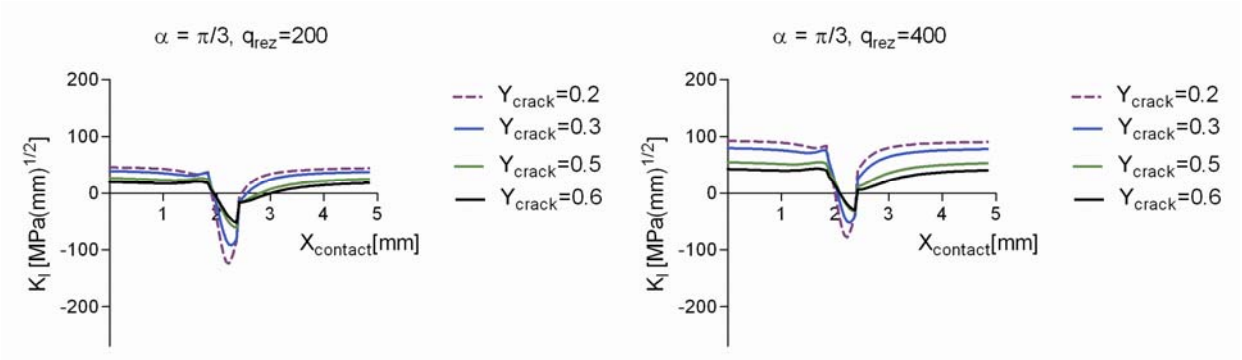
α = π/3, q_rez=200
α = π/3, q_rez=400
K_I [MPa(mm)^1/2]
X_contact[mm]
Y_crack=0.2
Y_crack=0.3
Y_crack=0.5
Y_crack=0.6

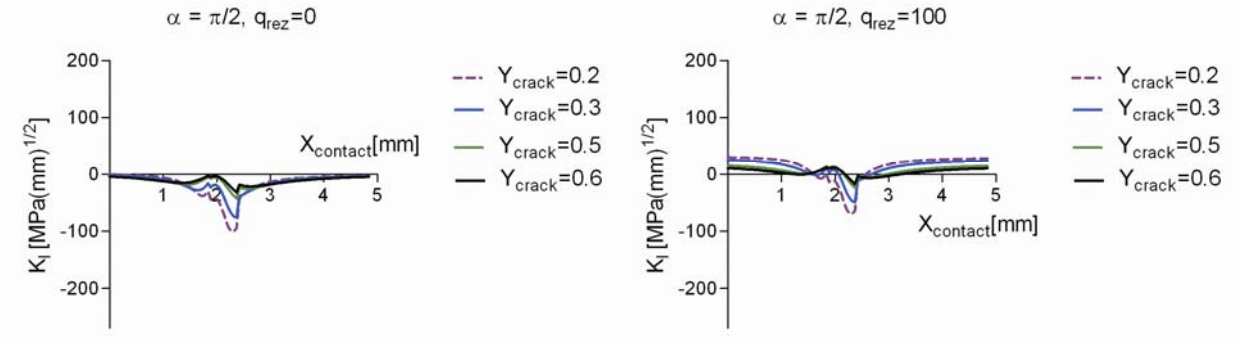
α = π/2, q_rez=0
α = π/2, q_rez=100
K_I [MPa(mm)^1/2]
X_contact[mm]
Y_crack=0.2
Y_crack=0.3
Y_crack=0.5
Y_crack=0.6

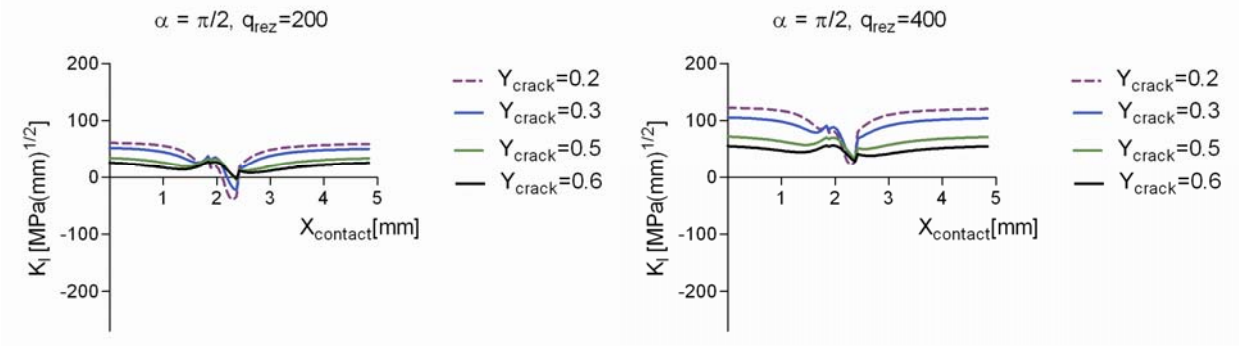
α = π/2, q_rez=200
α = π/2, q_rez=400
K_I [MPa(mm)^1/2]
X_contact[mm]
Y_crack=0.2
Y_crack=0.3
Y_crack=0.5
Y_crack=0.6

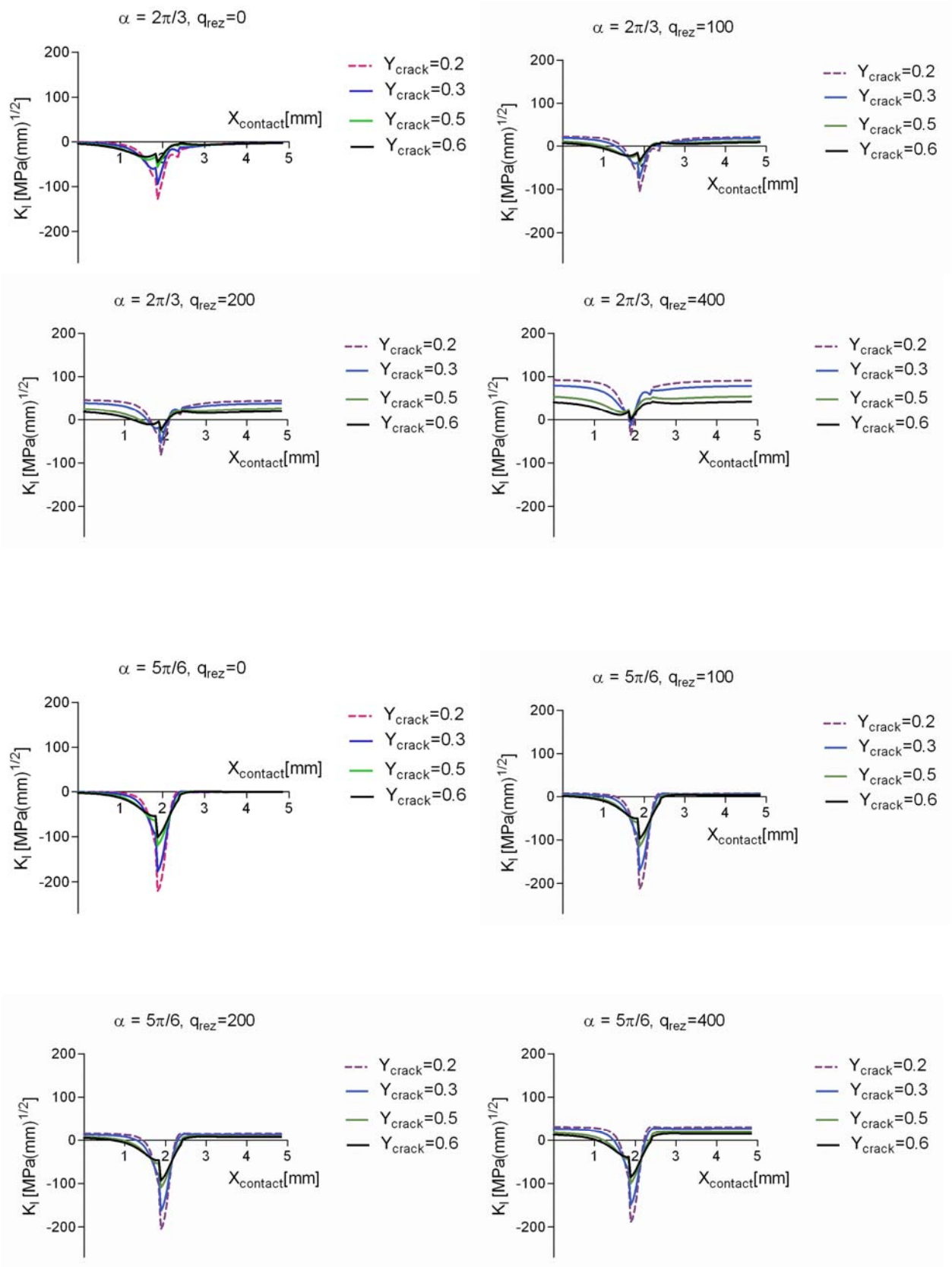

Fig. 5: SIF K_I variation as function of crack centre depth (Y_{crack}, mm) and residual tensions (q_{rez}, MPa)

5. CONCLUSIONS

For a more accurate life prediction of a fatigue crack, fracture mechanics considers that there are three stages that govern the fatigue behavior of the component, namely: crack initiation, long crack propagation and final fracture.

Stress intensity factor (SIF) is a sufficient parameter to describe the whole stresses field around the crack (in LEFM approaches) and can model the stable crack growth behavior.

Positive values of SIF mode I, K_I, can produce the crack growth by opening mode.

Due to the fact that in the contact zone, if there are no residual tensions, there are compressive stresses, K_I having negative values, the crack growth under Mode I (opening mode) is obstructed.

The residual tensions can produce tensile tensions in the contact zone, so the crack can grow under mode I.

The greater q_{rez}, the crack growth probability under Mode I is greater.

The maximum variation of K_I ($\Delta K_{I\ max}$) is obtained for Y_{crack} = 0.2 mm or, generally, if the crack is closer to the surface.

There are no influences of residual tensions (q_{rez}) for a crack parallel to the contact surface ($\alpha = 0$).

For the rest of the α angles, the K_I values are actually growing with q_{rez}.

For a small value of α angle we observed a small growth of K_I, but its value is increasing (reaching the minimum absolute value) with α growing, the maximum value being obtained for $\alpha = \pi/2$.

For the values of inclination angle of the internal crack $\alpha > \pi/2$, the growing of K_I values as function of q_{rez} are decreasing with the growing of α angles.

6. REFERENCES

[1] Anderson, T. L., (2005), *Fracture Mechanics, Fundamentals and Applications*, 3rd Edition, CRC, Taylor & Francis.

[2] Broek, D., (1984), *Elementary engineering fracture mechanics*, Martinus Nijhoff Publishers, Hague.

[3] Cioclov, D., (1977), *Mecanica ruperii materialelor*, Editura Academiei RSR, Bucureşti (in Romanian).

[4] Keer, L.M., Bryant, M.D. (1983), *A Pitting Model of Contact Fatigue*, ASME J. of Lubrication Technology, 105, p. 198-205.

[5] Kudish, I.I. (2000), *A New Statistical Model of Contact Fatigue*, Tribology Transactions, 43, 4, p. 711-721.

[6] McEvily, A.J., (1996), *Fatigue Crack Threshold*, ASM Handbook, Fatigue and Fracture, vol. 19, ASM International, p. 318-329.

[7] Murakami, K., (1987), *Stress Intensity Factor Handbook*, vols. I and II, Pergamon Press.

[8] Perez, N., (2004), *Fracture Mechanics*, Kluwer Academic Publishers, Boston.

[9] Ponomariov, S.D., Biderman V.L., Liharev, K.K. Makuşin, V. M., Malinin, N. N., Feodosiev, V. I., (1964) *Calculul de rezistență în construcția de maşini*, vol. II, Editura Tehnică, Bucureşti (in Romanian).

[10] Popinceanu, N., Gafițanu, M., Diaconescu, E., Crețu, S., Mocanu, D.R., (1985), *Problemele fundamentale ale contactului cu rostogolire*, Editura Tehnică, Bucureşti (in Romanian).

[11] Sauer, L., (1970), *Angrenaje. Proiectare. Materiale,* Editura Tehnică, Bucureşti (in Romanian).

[12] Saxena A., Muhlstein C.L., (1996), *Fatigue Crack Growth Testing*, ASM Handbook, Fatigue and Fracture, vol. 19, ASM International, p. 410-452.

[13] Tada, H., Paris, P., Irwin, G.R., (1973), *The Stress Analysis of Cracks Handbook*, Del Research Corporation.

[14] Tudose, L.M., Popa C.O., (2007), *Stress Intensity Factors Analysis on Cracks in the Hertzian Stresses Field of Teeth Gears*, ROTRIB 07, RO-118-1-8, ISSN 1843-6501.

[15] Tudose, L.M., Popa C.O., (2007), *Fatigue Crack Growth Simulation in the Hertzian Stresses Field of Teeth Gears*, ROTRIB 07, RO-066-1-9, ISSN 1843-6501.

[16] Tyron, R.G., (1997), *Probabilistic Mesomechanical Fatigue Model*, Grant NGT-51053, Lewis Research Center.